

Many-body open quantum systems beyond Lindblad master equations

Xiansong Xu,¹ Juzar Thingna,² Chu Guo,³ and Dario Poletti¹

¹EPD Pillar, Singapore University of Technology and Design, 8 Somapah Road, 487372 Singapore

²Complex Systems and Statistical Mechanics, Physics and Materials Science

Research Unit, University of Luxembourg, L-1511 Luxembourg, Luxembourg

³Zhengzhou Information Science and Technology Institute, Zhengzhou 450004, China

Many-body quantum systems present a rich phenomenology which can be significantly altered when they are in contact with an environment. In order to study such set-ups, a number of approximations are usually performed, either concerning the system, the environment, or both. A typical approach for large quantum interacting systems is to use master equations which are local, Markovian, and in Lindblad form. Here, we present an implementation of the Redfield master equation using matrix product states and operators. We show that this allows us to explore parameter regimes of the many-body quantum system and the environment which could not be probed with previous approaches based on local Lindblad master equations.

Introduction. In quantum systems, interactions can induce phases of matter with peculiar properties [1]. While it is still a very demanding task to understand the ground state properties of strongly correlated quantum systems, the study of many-body quantum systems in contact with an environment is a much less explored territory. In this case the environment can significantly alter the properties of the system, either suppressing desired properties or enhancing them [2, 3]. For example, the environment can induce dephasing in a system, thus forcing it to lose coherence, or to alter or suppress its localization properties [4–12]. On the other hand, a bath, especially if carefully tailored, can be used to favor condensation [2, 13] or exotic phases of matter in the steady state [3] or for long times [14, 15]. The interplay of strong interaction and dissipation has also been shown to result in non-trivial relaxation regimes, from power-law [16, 17] to stretched exponentials [5, 6, 18] and aging [19]. For a review on some aspects of many-body open quantum system one can refer to [20]. The study of such systems is however limited by approximations needed to treat the many-body quantum system and to model the environment and its interaction with the system itself.

The difficulty of studying many-body quantum systems (even when isolated from the environment) stems from the fact that a many-body wave function lives in a space which grows exponentially with the system size. Hence, simulation of such systems would be computationally expensive, even for a few tens of sites. Over the years, various numerical methods have been developed to study such systems, from mean field [21–26], to dynamical mean-field theory [27–29] and quantum Monte Carlo [30–32]. Another family of methods uses tensor networks [33–36], especially for one dimensional systems where they are commonly known as matrix product states (MPSs). In this scenario, tensor network algorithms are implemented in different flavours to search for ground states, [37] and to compute time evolutions [38–42].

For open quantum systems the computational complexity grows further. In fact, density matrices are described in a space which is the square of that of wave functions. Moreover, the environments need to be modeled appropriately for an accurate description of dissipative effects. For weak system-

environment coupling, it is possible to derive various master equations under different assumptions [43–45].

Current studies of large many-body open quantum systems mostly rely on master equations in Lindblad form [46, 47] due to its ease of implementation and computation. In addition, to study large systems, further assumption on the locality of operators used is required in order to remove the time dependence in the dissipator. However, they may not produce physical results even for weak system-environment coupling [48–51]. To go beyond the local system operator assumption, one could opt for master equations with a global system operator. Unfortunately, however, these master equations usually work in eigenbasis where the full energy spectra are required, making it difficult to simulate large quantum systems. Hence, it has not been shown how to simulate large many-body quantum systems with master equations that go beyond the local Lindblad approach. Due to these constraints, a large variety of many-body open quantum systems still remains unexplored.

Here we show how to realize the Redfield master equation RME, which goes beyond the limits of local Lindblad master equations, by using matrix product states to study larger many-body quantum systems. As an application, we consider an XXZ spin chain with its center site coupled to a thermal bath and we show the system’s response to the thermal bath by analysing the local magnetization and correlation propagation. We also demonstrate that this approach goes beyond various Lindblad master equation approaches.

Framework. We consider a time-independent total Hamiltonian H_{tot} including both the system and bath

$$H_{\text{tot}} = H_S + H_B + S \otimes B, \quad (1)$$

where H_S is the Hamiltonian of the system under consideration, H_B is the bath Hamiltonian, and the interaction between system and bath is given by $S \otimes B$ where S acts on the system while B acts on the bath. Assuming the system-bath coupling to be weak, and that the initial global density matrix of the system and bath $\rho_{\text{tot}}(0)$ is in a separable form $\rho_{\text{tot}}(0) \approx \rho(0) \otimes \rho_B$ where the reduced density matrix $\rho(0)$ describes the system while ρ_B is a thermal Gibbs state for the bath at temperature T , it is possible to derive a master equa-

tion for the evolution of $\rho(t)$ given by

$$\frac{\partial \rho(t)}{\partial t} = -i[H_S, \rho(t)] + \mathcal{R}^t[\rho(t)], \quad (2)$$

which is also known as the Redfield master equation (RME) [52]. Here the first term on the right-hand side describes the unitary evolution due to the system Hamiltonian. The dissipation due to the bath is described by a time-dependent superoperator

$$\mathcal{R}^t[\cdot] = [\mathbb{S}(t) \cdot, S] + [S, \cdot \mathbb{S}^\dagger(t)], \quad (3)$$

$$\mathbb{S}(t) = \int_0^t \tilde{S}(-\tau) C(\tau) d\tau, \quad (4)$$

with $\tilde{S}(\tau) = e^{iH_S\tau} S e^{-iH_S\tau}$ while the bath correlation function is $C(\tau) = \text{tr}(e^{iH_B\tau} B e^{-iH_B\tau} B \rho_B)$. Note that we work in units such that $J = \hbar = k_B = 1$, where k_B is the Boltzmann constant.

To simulate quantum dynamics by using Eq. (2), one would typically diagonalize the system Hamiltonian H_S and express the terms of (3) in the energy eigenbasis. Such an approach strongly limits the size of the systems that can be studied. For the long time dynamics or steady states, one could evolve the system under a time-independent dissipator $\mathcal{R}^\infty[\cdot]$ with the transition operator $\mathbb{S}(\infty)$. For clarity, we refer to it as the time-independent Redfield master equation (iRME) in contrast to the time-dependent one in Eq.(2).

In order to investigate larger systems, Lindblad master equation with short range operators are typically used. The advantage of such a master equations is that they can be simulated very effectively with MPS algorithms, either using a trajectory method [20, 53] or the purification of the density matrix [41]. A common microscopic derived Lindblad master equation with local operators relies on the local Hamiltonian approximation and a high temperature condition [48], and it is known as the local Lindblad master equation (LLME). In this case, the transition operator $\mathbb{S}(\infty)$ is governed by an approximated local system Hamiltonian (i.e., with inter-site coupling terms ignored).

Another archetypal approximation is to take the singular coupling limit master equation (SCME) [54, 55]. In this limit, the correlation function is approximated as $C(\tau) \approx 2a\delta(\tau)$ where a depends on the bath model. The corresponding transition operator $\mathbb{S}(\infty)$ then reduces to aS and as a result, the dissipator $\mathcal{R}^\infty[\cdot]$ becomes local and in Lindblad form too, thus allowing efficient evolution with MPSs.

Redfield dynamics with matrix product states. In order to accurately compute the evolution of a many-body open quantum system, it would be useful to develop a way to compute Eq. (2) with MPSs, which would allow to significantly increase the size of the systems currently studied by diagonalizing the system Hamiltonian H_S . In the following we explain how this can be done. It is possible to describe wave functions and density matrices, even exactly, as a product of tensors [35] with 3 indices, one for the physical dimension (e.g., of the size of the local Hilbert space), and two auxiliary dimensions (of a

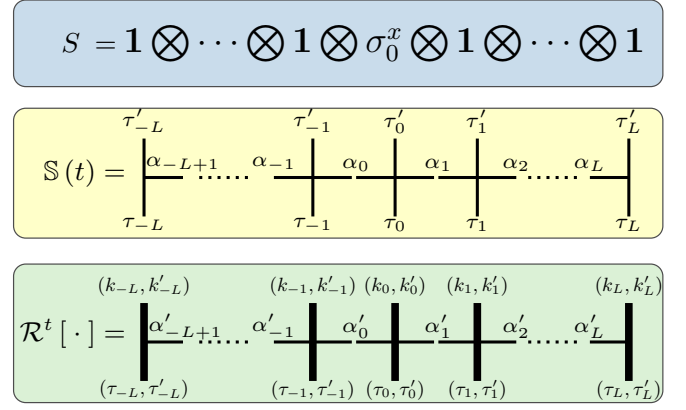


FIG. 1: Illustration of the MPO representation of $\mathbb{S}(t)$ and \mathcal{R}^t . Starting from the system–bath coupling operator S we evaluate $\mathbb{S}(t)$ via Eq. (4) and \mathcal{R}^t via Eq. (3). At site l the physical indices of the MPO tensor for \mathbb{S} are τ_l and τ'_l , while the auxiliary indices are α_l and α_{l+1} . For \mathcal{R}^t the tensor at site l has physical indices given by the tuples (τ_l, τ'_l) for the input and (κ_l, κ'_l) for the output, while the auxiliary indices are α'_l and α'_{l+1} .

maximum size called the bond dimension D). Operators acting on a state can be described by linear maps from MPS to MPS, which are called matrix product operators (MPOs). An MPO is a tensor with 4 indices, one for the input and one for the output physical dimensions, and two auxiliary dimensions of maximum size D_W (the MPO bond dimension). We first rewrite the system density matrix $\rho(t)$ as an MPS [41], and the operators acting on it as MPOs. The MPO representing S is then evolved in time to obtain $\tilde{S}(\tau)$ using a Trotter decomposition at second order. The convolution in Eq. (4) to compute \mathbb{S} is evaluated subsequently using Romberg integration. The algorithm to evaluate \mathcal{R}^t is described pictorially in Fig. 1. After having obtained \mathcal{R}^t we can use the Runge-Kutta method to evolve $\rho(t)$ using Eq. (2) [56].

Model. The methods described above could be applied to a broad range of physical systems. Here we consider a spin-1/2 Heisenberg XXZ spin chain with $(2L + 1)$ sites, with

$$H_S = \sum_{l=-L}^{L-1} [J(\sigma_l^x \sigma_{l+1}^x + \sigma_l^y \sigma_{l+1}^y) + \Delta \sigma_l^z \sigma_{l+1}^z] + h \sum_{l=-L}^L \sigma_l^z,$$

where h is a uniform magnetic field, and the elements of σ_l^α are given by the Pauli matrices for $\alpha = x, y, \text{ or } z$. J and Δ denote the tunneling strength and interaction strength respectively [57]. The central site ($l = 0$) of the spin chain is coupled to a harmonic oscillator bath, with bath Hamiltonian $H_B = \sum_{n=1}^{\infty} \left[\frac{p_n^2}{2m_n} + \frac{m_n \omega_n^2 x_n^2}{2} \right]$, through the system operator $S = \sigma_0^x$ and $B = -\sum_{n=1}^{\infty} c_n x_n$ where c_n is the system-bath coupling constant for the n -th mode. The bath properties can be characterized by the spectral function $J(\omega)$ [58]. In the following, we consider an ohmic bath with an exponential cutoff (i.e., $J(\omega) = \gamma \omega \exp(-\omega/\omega_c)$) [45, 58], and where $\gamma(\propto \sum_n c_n^2)$ is the dissipation strength. It follows that in the singular coupling limit the prefactor $a = \gamma T$. We consider a

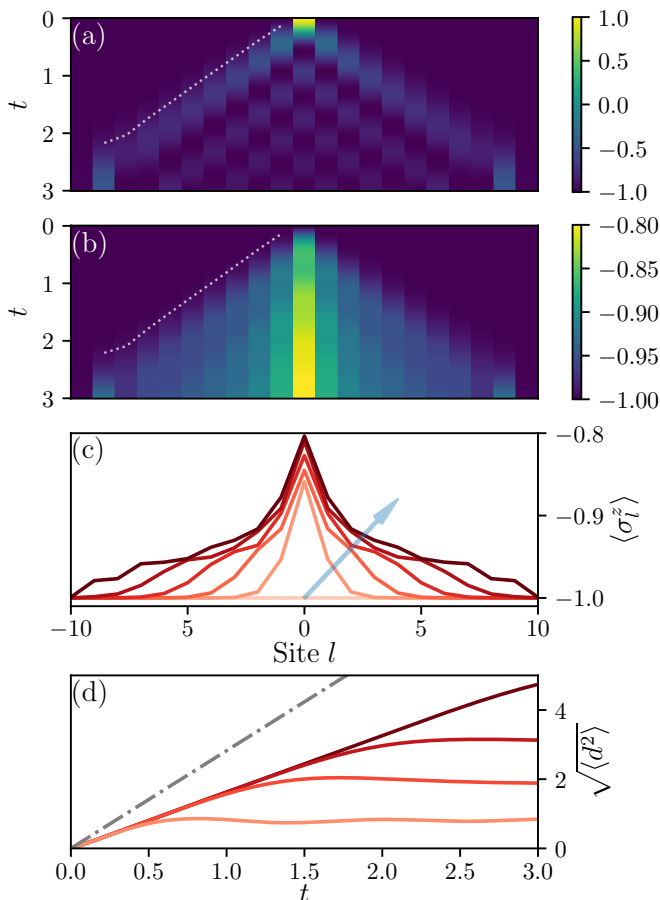


FIG. 2: (a) Contour plot of the local magnetization $\langle \sigma_l^z \rangle$ for a closed system with the central spin flipped initial state. (b) Contour plot of $\langle \sigma_l^z \rangle$ with Redfield master equation (2). (c) Local magnetization profile for times $t = 0, 0.5, 1, 1.5, 2, 2.5$ (darker lines for larger times). (d) $\sqrt{\langle d^2 \rangle}$ as a function of time for unitary dynamics (grey dash-dotted line), for 21 sites, and from Eq. (2) (red solid lines), for sizes 5, 9, 13 and 21 (darker lines for larger systems). Other parameters: $\Delta = 5, h = 0.5, \omega_c = 20, T = 2, \gamma = 0.02$.

system with 21 sites, i.e., $L = 10$, which cannot be simulated via conventional Redfield master equation approaches ($L \approx 4$ that is 9 – 10 sites at most). As initial condition we chose a fully polarized initial state $|\Psi_0\rangle = |\downarrow\downarrow\downarrow \cdots \downarrow\downarrow\downarrow\rangle$ which is an eigenstate of the system Hamiltonian and it only evolves due to the coupling to the bath.

Results. Since we couple the central spin to a bath that tends to flip it, we first study the dynamics of a flipped spin in such system, i.e. $|\Psi_U\rangle = |\downarrow \cdots \downarrow \uparrow \downarrow \cdots \downarrow\rangle$. This is represented in Fig. 2(a) where the local magnetization is shown to propagate, as expected, ballistically in the system with some modulations due to interference. In Fig. 2(b) we show the open system dynamics for the fully polarized state $|\Psi_0\rangle$, in which, on top of the linear propagation, there is a non-unitary dynamics in the center of the chain. This is shown more clearly in Fig. 2(c) which shows cuts, at different times, of panel (b). The dotted lines in Fig. 2(a,b) are computed from the data in Fig. 2(a), showing that the tails in the dissipative dynamics spread at

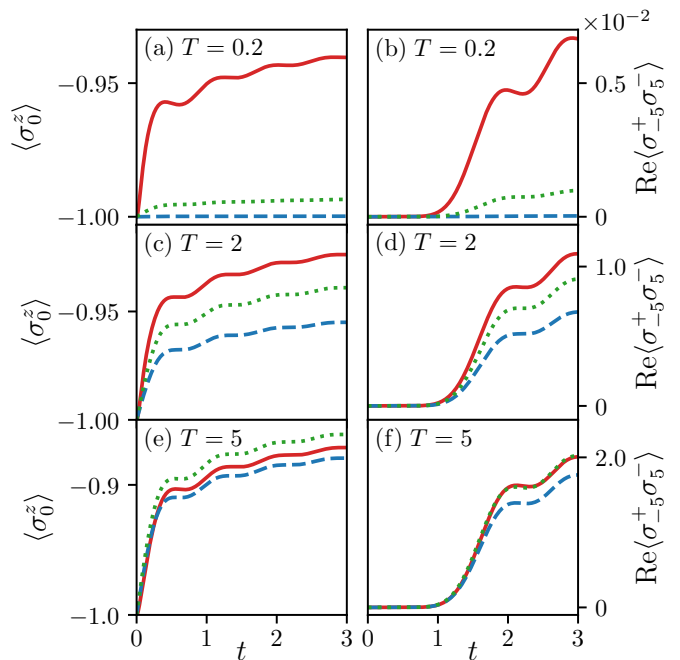


FIG. 3: Evolution of local magnetization $\langle \sigma_0^z \rangle$, panels (a,c,e) and real part of the long distance correlation $\langle \sigma_{-5}^+ \sigma_5^- \rangle$, panels (b,d,f) as functions of time. The evolutions are computed using RME (red solid lines), SCME (green dotted lines) and LLME (blue dashed lines) master equations. Panels (a,b) are for $T = 0.2$, (c,d) are for $T = 2$ and (e,f) are for $T = 5$. Other parameters: $\Delta = 0.5, h = 0.5, \omega_c = 20, \gamma = 0.02$.

the same speed as the unitary evolution. For a more quantitative comparison we study the variance of the spreading of the magnetization, given by

$$\langle d^2 \rangle = \sum_l \langle \sigma_l^u \rangle l^2 / \sum_l \langle \sigma_l^u \rangle, \quad (5)$$

where $\sigma_l^u = \sigma_l^+ \sigma_l^-$ with $\sigma_l^\pm = (\sigma^x \pm i\sigma^y)/2$. For the unitary evolution $\sqrt{\langle d^2 \rangle}$ grows linearly (grey dot-dashed line). The behavior is also linear for the dissipative evolution, due to the fact that an excitation, after it is introduced by the bath, propagates ballistically. For the dissipative evolution we have considered different system sizes so as to show how quickly finite size effects can play an important role and limit the predictive power.

We now compare the results of our approach to those of the LLME and SCME. We study two quantities, the local magnetization in the center $\langle \sigma_0^z \rangle$, Fig. 3(a,c,e), and the correlation between two distant sites $\langle \sigma_{-5}^+ \sigma_5^- \rangle$, Fig. 3(b,d,f), for different bath temperatures T . For low temperatures, Fig. 3(a,b), the dynamics of the Lindblad master equations (dashed blue line for LLME and green dotted line for SCME) is much slower than the more accurate RME (red continuous line). In fact, the derivation of both LLME and SCME requires a high temperature approximation. As T increases the curves approach each other, but even for $T = 5$, while the evolution is similar, the difference between the various Lindblad master equations

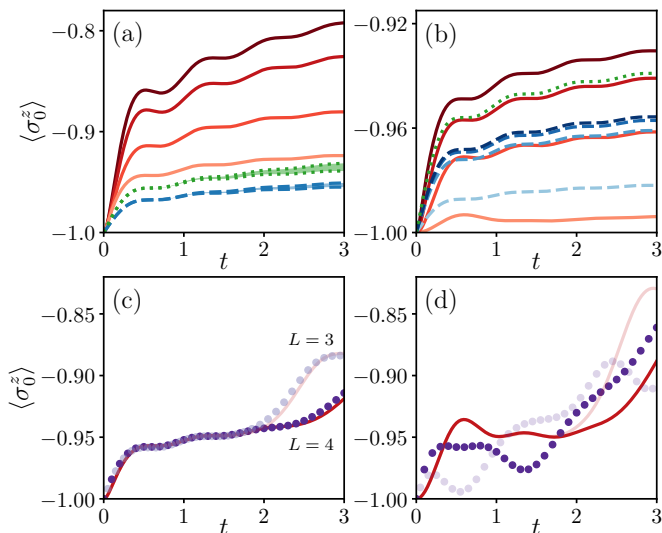


FIG. 4: Local magnetization $\langle \sigma_0^z \rangle$ versus time t (a) for different interactions $\Delta = 0.5, 1.5, 3, 5$ at $\omega_c = 20$ or (b) for different cut-off frequencies $\omega_c = 1, 5, 10$ at $\Delta = 0.5$, computed from RME (red solid lines with color gradient), SCME (green dotted lines), LLME (blue dashed lines) for 21 sites with $\gamma = 0.02$. Darker colors imply larger interactions or cut-off frequencies. (c,d) $\Delta = 0.5, \omega_c = 1, 10$ with $\gamma = 0.2, 0.02$ respectively to show comparable dynamics for RME (red solid lines), iRME (purple filled circles), for 7 sites (faint colors) and 9 sites (darker colors). In all panels, $T = 2$.

and RME is sizeable.

It is important to probe the performance of these master equations for varying many-body interaction strength Δ . In Fig. 4(a) we show the local magnetization $\langle \sigma_0^z \rangle$ versus time as we vary Δ . We observe that the dynamics is strongly affected by Δ (red continuous lines from light to dark as Δ increases), however the evolution of both Lindblad master equations does not vary significantly with Δ , but only changes in the shaded regions. This implies that these Lindblad master equations are unable to accurately capture the effect of strong interaction effectively approximating the many-body physics in this system.

We also study the effect of bath cutoff frequency ω_c , which modifies how different energy levels are coupled to the bath. In Fig. 4(b) we show $\langle \sigma_0^z \rangle$ as function of t for various cut-off frequencies ω_c . The SCME cannot probe the differences in ω_c . The LLME can vary with ω_c but it is not accurately reproducing the RME. It is also important to point out that, in the small ω_c regime, the evolution due to the time-dependent RME cannot be approximated by the (time-independent) iRME. This is highlighted in Fig. 4(c, d) where results from RME (red solid lines) are compared to those of its time-independent approximation iRME where \mathcal{R}^∞ is used instead of \mathcal{R}^t (purple circles) [59]. For small enough cut-offs ω_c the finite time effects are stronger and the inaccuracy of the iRME more evident. This is due to the fact that at small frequencies the size of the system plays a bigger role. For the iRME the superoperator \mathcal{R}^∞ would straight-away be affected

by the finite system size, while \mathcal{R}^t would require some time before the finite size effects are felt.

Conclusions. We have presented an implementation of the Redfield master equations using MPS/MPOs. Unlike the conventional approach that requires the full eigenenergy spectrum, the MPS/MPO-based method allows us to probe the dynamics of large many-body open quantum systems. We have compared results from the Redfield master equation to typical master equations in Lindblad form which can be computed efficiently for large systems, and we have shown that those Lindblad master equations do not capture the dynamics as the Redfield master equation can. Moreover, the time-dependence in the evolution equations of our approach does not come at an additional cost and in most of the regimes it is computationally cheaper than the time-independent counterpart. The approach is thus robust and the current algorithm can be readily extended to the study of multiple baths, different types of couplings, or even systems with time-dependent Hamiltonians.

More work would be needed to increase the efficiency of the code, especially in terms of memory requirements, for example using different evolution or integration schemes. Comparison to the MPS approach used in [60–62], which is also valid for strong system-bath coupling, would give important insights in the regime of validity of the weak coupling approximation [63, 64].

The possibility of studying accurately the open dynamics of many-body quantum systems beyond Lindblad master equations leads to interesting opportunities in various directions, for instance quantum thermodynamics and quantum transport.

Acknowledgments. D.P. acknowledges fruitful discussions with S. Maniscalco and K. Modi. D.P. and X.X. acknowledge support from Ministry of Education of Singapore AcRF MOE Tier-II (project MOE2016-T2-1-065, WBS R-144-000-350-112). C.G. acknowledges support from National Natural Science Foundation of China (11504430). J.T. acknowledges support from European Research Council project NanoThermo (ERC-2015-CoG Agreement No. 681456). This research was supported in part by the National Science Foundation under Grant No. NSF PHY-1748958. The computational work for this article was partially performed on resources of the National Supercomputing Centre, Singapore (<https://www.nsc.sg>).

-
- [1] S. Sachdev, *Quantum Phase Transitions*, Cambridge University Press (2011).
 - [2] S. Diehl, A. Micheli, A. Kantian, B. Kraus, H. P. Büchler, and P. Zoller, Nat. Phys. **4**, 878 (2008).
 - [3] M. Müller, S. Diehl, G. Pupillo, and P. Zoller, Adv. At. Mol. Opt. Phys. **61**, 1 (2012).
 - [4] M. H. Fischer, M. Maksymenko, and E. Altman, Phys. Rev. Lett. **116**, 160401 (2016).
 - [5] E. Levi, M. Heyl, I. Lesanovsky, and J. P. Garrahan, Phys. Rev. Lett. **116**, 237203 (2016).

- [6] B. Everest, I. Lesanovsky, J. P. Garrahan, and E. Levi, Phys. Rev. B **95**, 024310 (2017).
- [7] M. Žnidarič, J. J. Mendoza-Arenas, S. R. Clark, and J. Goold, Ann. Phys. (Berlin) **529**, 1600298 (2017).
- [8] M. Žnidarič, A. Scardicchio, and V. K. Varma, Phys. Rev. Lett. **117**, 040601 (2016).
- [9] M. V. Medvedyeva, T. Prosen, and M. Žnidarič, Phys. Rev. B **93**, 094205 (2016).
- [10] E. P. L. van Nieuwenburg, J. Yago Malo, A. J. Daley, and M. H. Fischer, Quantum Sci. Technol. **3**, 01LT02 (2018).
- [11] X. Xu, C. Guo, and D. Poletti, Phys. Rev. B **97**, 140201 (2018).
- [12] I. Vakulchyk, I. Yusipov, M. Ivanchenko, S. Flach, and S. Denisov, arXiv:1709.08882.
- [13] S. Diehl, A. Tomadin, A. Micheli, R. Fazio, and P. Zoller, Phys. Rev. Lett. **105**, 015702 (2010).
- [14] J.-S. Bernier, P. Barmettler, D. Poletti, and C. Kollath, Phys. Rev. A **87**, 063608 (2013).
- [15] T. Shirai, J. Thingna, T. Mori, S. Denisov, P. Hänggi, and S. Miyashita, New J. Phys. **18**, 053008 (2016).
- [16] D. Poletti, J.-S. Bernier, A. Georges, and C. Kollath, Phys. Rev. Lett. **109**, 045302 (2012).
- [17] Z. Cai and T. Barthel, Phys. Rev. Lett. **111**, 150403 (2013).
- [18] D. Poletti, P. Barmettler, A. Georges, and C. Kollath, Phys. Rev. Lett. **111**, 195301 (2013).
- [19] B. Sciolla, D. Poletti, and C. Kollath, Phys. Rev. Lett. **114**, 170401 (2015).
- [20] A. J. Daley, Adv. Phys. **63**, 77 (2014).
- [21] M. Gutzwiller, Phys. Rev. Lett. **10**, 159 (1963).
- [22] M. Gutzwiller, Phys. Rev. **134**, A923 (1964).
- [23] M. Gutzwiller, Phys. Rev. **137**, A1726 (1965).
- [24] M. P. A. Fisher, P. B. Weichman, G. Grinstein, and D. S. Fisher, Phys. Rev. B **40**, 546 (1989).
- [25] D. S. Rokhsar, and B. G. Kotliar, Phys. Rev. B **44**, 10328 (1991).
- [26] D. Jaksch, C. Bruder, J. I. Cirac, C. W. Gardiner, and P. Zoller, Phys. Rev. Lett. **81**, 3108 (1998).
- [27] W. Metzner, and D. Vollhardt, Phys. Rev. Lett. **62**, 324 (1989).
- [28] A. Georges and G. Kotliar, Phys. Rev. B **45**, 6479 (1992).
- [29] A. Georges, G. Kotliar, W. Krauth, and M. J. Rozenberg, Rev. Mod. Phys. **68**, 13 (1996).
- [30] G. Senatore, and N. H. March, Rev. Mod. Phys. **66**, 445 (1994).
- [31] D. M. Ceperley, Rev. Mod. Phys. **67**, 279 (1995).
- [32] W. M. C. Foulkes, L. Mitos, R. J. Needs, and G. Rajagopal, Rev. Mod. Phys. **73**, 33 (2001).
- [33] U. Schollwöck, Rev. Mod. Phys. **77**, 259 (2005).
- [34] F. Verstraete, V. Murg, and J.I. Cirac, Adv. Phys. **57**, 143 (2008).
- [35] U. Schollwöck, Ann. Phys. **326**, 96 (2011).
- [36] R. Orús, Ann. Phys. **349**, 117 (2014).
- [37] S. R. White, Phys. Rev. Lett. **69**, 2863 (1992).
- [38] S. R. White, and A.E. Feiguin, Phys. Rev. Lett. **93**, 076401 (2004).
- [39] G. Vidal, Phys. Rev. Lett. **93**, 040502 (2004).
- [40] A. J. Daley, C. Kollath, U. Schollwöck, and G. Vidal, Jour. Stat. Mech. Th. Exp. P04005 (2004).
- [41] F. Verstraete, J. J. García-Ripoll, and J. I. Cirac, Phys. Rev. Lett. **93**, 207204 (2004).
- [42] M. Zwolak, and G. Vidal, Phys. Rev. Lett. **93**, 207205 (2004).
- [43] C. W. Gardiner and P. Zoller, *Quantum Noise* (Springer-Verlag, Berlin, Heidelberg, 2000).
- [44] H.-P. Breuer and F. Petruccione, *The theory of open quantum systems*, (Oxford University Press, Oxford, 2002).
- [45] I. de Vega and D. Alonso, Rev. Mod. Phys. **89**, 015001 (2017).
- [46] V. Gorini, A. Kossakowski, and E.C.G. Sudarshan, J. Math. Phys. **17**, 821 (1976).
- [47] G. Lindblad, Commun. Math. Phys. **48**, 119 (1976).
- [48] H. Wichterich, M. Henrich, H.-P. Breuer, J. Gemmer, and M. Michel, Phys. Rev. E **76**, 031115 (2007).
- [49] A. Purkayastha, A. Dhar, and M. Kulkarni, Phys. Rev. A **93**, 062114 (2016).
- [50] X. Xu, J. Thingna, and J.-S. Wang, Phys. Rev. B **95**, 035428 (2017).
- [51] A. Levy and R. Kosloff, Europhys. Lett. **107**, 20004 (2014).
- [52] A. G. Redfield, IBM J. Res. Dev. **1**, 19 (1957).
- [53] K. Molmer, Y. Castin, and J. Dalibard, Jour. Opt. Soc. Am. B **10**, 030525 (1992).
- [54] V. Gorini and A. Kossakowski, J. Math. Phys. **17**, 1298 (1976).
- [55] P. F. Palmer, J. Math. Phys. **18**, 527 (1977).
- [56] In all our simulations we use maximum bond dimensions $D = 100$ and $D_W = 30$. The time step in the second order Trotter evolution of the MPO is 0.00125, and in the 4th order Runge-Kutta evolution of the density matrix, is 0.01. For the Romberg integration we use a 3rd order with time step 0.00125. For the evolution of Lindblad master equations we use $D = 100$ with 4th order Trotter-Suzuki method with time step 0.01.
- [57] We note here that the presence of a local magnetization h is a prerequisite for LLME to perform a local approximation, while it is not necessary for RME.
- [58] From the definition of $C(\tau)$ we get $C(\tau) = \int_0^\infty (d\omega/\pi) J(\omega) [\coth(\omega/2T) \cos(\omega\tau) - i \sin(\omega\tau)]$ with $J(\omega) = \pi \sum c_n^2 / (2m_n \omega_n) \delta(\omega - \omega_n)$.
- [59] In our approach it is effectively easier to compute the evolution for RME rather than iRME due to a integration up to infinite time t . Hence for this panel we study a smaller system.
- [60] I. de Vega, and M.-C. Banuls, Phys. Rev. A **92**, 052116 (2015).
- [61] C. Guo, I. de Vega, U. Schollwöck, and D. Poletti, Phys. Rev. A **97**, 053610 (2018).
- [62] C. Cascio, J. C. Halimeh, I. P. McCulloch, A. Recati, and I. de Vega, arXiv:1801.08176
- [63] J. Thingna, J.-S. Wang, and P. Hänggi, J. Chem. Phys. **136**, 194110 (2012).
- [64] J. Thingna, J.-S. Wang, and P. Hänggi, Phys. Rev. E **88**, 052127 (2013).